

## Internal morphology of mineral crystals as clue to their growth histories. I. Growth kinematics

*Ilia Vesselinov*

**Abstract.** Measurements of edge trajectories (sector boundaries) in oriented crystal sections provide quantitative information about the growth histories of minerals but the methods for deriving and analyzing such data are poorly developed. This study treats internal morphological patterns in terms of an inverse problem in growth kinematics and describes a procedure for computer modelling of measured patterns. Edge trajectories, which record the variations of growth rate ratios of adjacent faces in time, are modelled by four types of absolute rate functions representing decelerating, constant-rate, accelerating and oscillatory growth modes. They are illustrated with analyses of the few measured patterns available in the literature. Straight trajectories like those described in accessory zircon from granitoids demonstrate the evolution of stationary growth forms during mineral formation. A hyperbolic pattern recorded in authigenic albite from limestone illustrates processes which do not produce stationary forms. A parabolic hourglass structure in titanite phenocryst demonstrates the significance of internal growth morphologies for understanding the processes in magma bodies. Oscillatory patterns are natural time-scaling indicators and, in addition, structures like that in a crystal of hydrothermal arsenopyrite provide key information about related compositional variations. Growth kinematics of crystals provides abundant clues constraining the inferred conditions of mineral formation.

*Key words:* crystal growth, kinematics, sector zoning

*Address:* Geological Institute, Bulgarian Academy of Sciences, 1113 Sofia, Bulgaria; e-mail: ivess@geology.bas.bg

В е с е л и н о в, И. 1998. Вътрешната морфология на кристалите на минералите като индикатор на процесите на растежа им. I. Кинематика. - *Геохим., минерал. и петрол.*, **34**, 3-14

Измерването на траекториите на кристалните ръбове (секторните граници) в ориентирани прерези дава количествена информация за растежа на минералите, но методите за извличане и анализирание на такива данни са слабо развити. Настоящата работа разглежда вътрешните морфоложки структури в рамките на една обратна кинематична задача и предлага процедура за компютърното им моделиране. Ръбните траектории, фиксирани измененията на отношенията на абсолютните скорости на съседните стени във времето, се моделират посредством четири типа функции в режими на намаляващи, постоянни, растящи и периодично изменящи се скорости на растеж. Те са илюстрирани с анализи на малкото измерени структури, публикувани в литературата. Праволинейните траектории, като описаните в акцесорния циркон от гранитоиди, показват еволюцията на стационарните форми на растеж при минералообразуването. Една хиперболична структура, описана в аутигенен албит от варовици, илюстрира процеси, при които стационарни форми не се образуват. С една параболична структура в порфирен титанавгит е показано значението на вът-

решната морфология за тълкуване на процесите в магмени тела. Осцилационните траектории са естествени "часовници" и освен това структури като тази в един кристал на хидротермален арсенипит дават ключова информация за свързаните със скоростта на растеж изменения в състава. В кинематиката на кристалния растеж се крият обилни данни за тълкуване на условията на минералообразуване.

*Ключови думи:* кристален растеж, кинематика, секторна зоналност

*Адрес:* Геологически институт, Българска академия на науките, 1113 София

## Introduction

Mineral kinetics has increasingly drawn the attention of researchers during the recent years and voluminous information has been gained by studying the internal inhomogeneities of mineral crystals. So far, however, the efforts have been concentrated on their compositional characteristics, size distributions, etc. (e.g. Holten et al., 1997; Cashman, 1990) while the geometry of patterns, such as those of concentric and sector zoning, has been largely neglected. It is well known (Sunagawa, 1987) that both types of zoning reflect the evolution of crystal shapes during growth and that an external morphology can be treated as formed of the bases of growth pyramids whose lateral surfaces extend into the interior along the trajectories of crystal edges producing an internal morphological pattern from which the geometry of a crystal can be traced back in time to its origin. In 1948, Laemmlein derived the basic relation of internal morphology in the form  $V_y/V_x = \sin\psi_y/\sin\psi_x$  where  $V_y, V_x$  are the growth rates of any two adjacent flat faces of a crystal along their normals at a given moment, and  $\psi_y, \psi_x$  are the angles which they make with the common surface of their growth pyramids and which, in sections perpendicular to the zone axis, are the angles between the face projections and the trajectory of the interfacial edge during growth. Since edge paths in crystal sections can be measured in many mineral specimens, it may be seen that Laemmlein's relation shows the means of gaining direct quantitative information about crystal growth kinematics as a basis for a better understanding of growth kinetics, i.e. of the factors that governed mineral crystallization in processes of the past. It should be emphasized again that few studies, to be discussed further on, have made limited use of that important source of

information. As a result, the description and analysis of kinematic patterns are still poorly developed.

In a previous study (Vesselinov, 1997), a procedure has been proposed for routine preparation of crystal sections perpendicular to desired zone axes. Measurements of edge trajectories in such oriented sections overcome a serious problem in quantifying internal morphologies and permit to study them on the basis of Laemmlein's relation. As will be shown, however, a meaningful analysis of such data requires tests of various growth hypotheses producing morphologies to be compared with the measured patterns, i.e. one should be able to „grow“ hypothetical crystals using the kinematic information derived. For the purpose the SHAPE 5.0 crystal-drawing computer program of Dowty (1995) has been used as an invaluable tool in this study. Its option „Sections and Growth Rates“ is designed exactly for this kind of problems and has made it possible to model and illustrate all kinematic patterns discussed here.

The first part of this study presents an analysis of internal morphological patterns in terms of an inverse problem in growth kinematics and tries to generally outline the scope of information that can be gained by measuring the patterns and expressing edge paths in quantitative terms. The second part examines some kinetic implications of kinematic results.

## Edge trajectories and their measurement

Obviously, in order to be measured edge paths should first be made visible in the given crystal section. Present-day techniques (optical microscopy, BSE-imaging, cathodoluminescence, etching, etc.) open up many possible ways of exposing or trac-

ing out edge paths, and in the following the latter will be treated as fully exposed. It should be noted that the degree of exposure itself contains information about the absolute rates at which growth has taken place. This is illustrated in Fig. 1a,b,c which is a sketch of three cases commonly observed in BSE-images of compositional inhomogeneities. Fig. 1a shows a perfectly homogeneous section with non-observable edge paths, in Fig. 1b a homogeneous core is surrounded by a zoned rim with traceable edge paths along the successive corners of time-equivalent zones, and in Fig. 1c the rim shows well defined sector boundaries between symmetrically non-equivalent faces. As will be shown in Part II of this study, the presence or absence of sector boundaries in a section puts valid constraints on the absolute growth rates of the crystal which in this example, under otherwise equal conditions, would be higher in Fig. 1c than in Fig. 1a,b.

All trajectories are treated here (Fig. 1d) as starting from the original seed where growth began at zero time. In practice, however, section planes cut the growth pyramid structure either below or above its origin exposing only parts of the edge path patterns along the perpendicular zone axes and the position of the origin in such cases is poorly defined. For this reason, external outlines of sections generally provide a better frame of reference and it is recommendable to measure patterns from the outline towards the centre of sections. Laemmlein's relation also uses the angles with the face projections rather than those with the face normals. Such a procedure would require recalculation of measured values to bring them to a common origin but this technical problem will not be discussed.

The shapes of edge trajectories, whole or partial, may be conveniently grouped into three categories: straight, curved and undulating (Fig. 1d). They are defined at any point by Laemmlein's angles  $\psi_y$ ,  $\psi_x$  related as  $\psi_x + \psi_y = 180 - \phi$ , where  $0 < \phi < 180$  is the interfacial angle of the faces x,y. Laemmlein's relation means that the trajectory curves away from the slower growing face (Laemmlein, 1948) and that at  $\psi_x = 0$  the face x stops growing whereas at

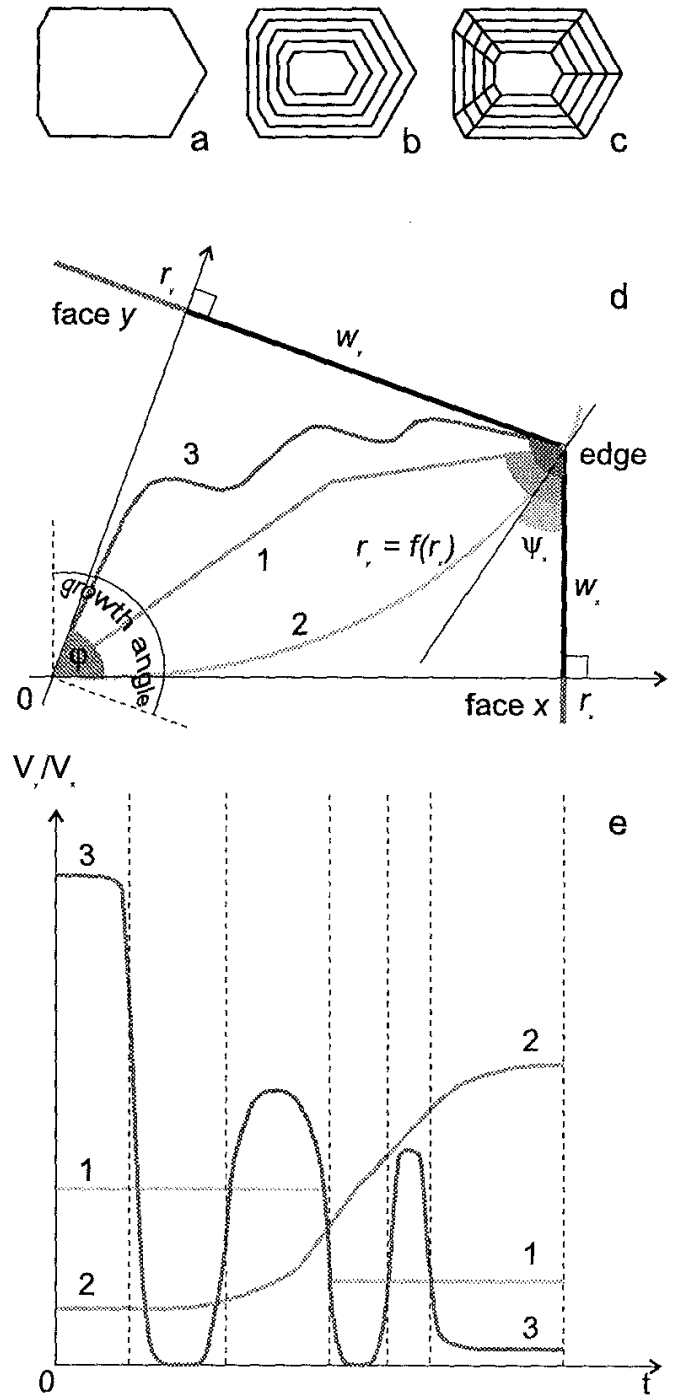


Fig. 1. Sections, edge trajectories and their significance: a - homogeneous section; b - traceable edge paths; c - sector boundaries between faces not related by symmetry; d - straight (1), curved (2) and undulating (3) edge trajectories; e - growth events marked by the changes of directions of edge paths

Фиг. 1. Прерези, ръбни траектории и значението им: a - еднороден пререз; b - ръбни траектории, маркирани от концентрична зоналност; c - секторни граници между стени, несвързани със симетрични елементи; d - праволинейни (1), криволинейни (2) и вълновидни (3) ръбни траектории; e - събития по време на растежа, маркирани от промените в посоката на ръбните траектории

$\psi_x = (180 - \phi)$  the same happens with the face y. Since we discuss growth forms only, i.e.

their rates are  $V_x \geq 0$ ,  $V_y \geq 0$  at any moment, it follows  $0 \leq \psi_x \leq (180 - \varphi)$ , or  $(180 - \varphi) \geq \psi_y \geq 0$ . In Fig. 1d,  $(180 - \varphi)$  is designated as growth angle to emphasize the fact that it restricts the variations of the trajectory tangent during growth as well as the area of a section polygon within which the edge projection may advance. In Fig. 1e, the three types of internal morphological patterns are expressed in kinematic terms as follows from Laemmlein's equation. Any change in direction of these lines can be treated as marking some event in the growth history of the crystal, and the figure illustrates three entirely different sequences of events ending in identical external morphologies. An important case of edge path geometry is not illustrated here (examples may be seen in the section on oscillatory patterns) in order to avoid excessive details but it needs mentioning because it shows the effect of the relative magnitudes of growth angles on edge path patterns. If a face grows between two other faces and the sum of the two adjacent interfacial angles is smaller than 180, then the sum of the respective growth angles will be larger than 180 and they will overlap. The smaller the interfacial angles the larger the overlap of growth angles. Inside its area the two edge paths may meet, i.e. the face in between may disappear, to be replaced by a single-edge trajectory defined by the other two faces. Such an event (or inversely, the appearance of a new face between the two faces) will happen at a definite value of the rate ratio of the central face relative to the side faces marking a significant change in growth morphology. In a section polygon, the probability of coming across such events increases with the increasing number of faces in the zone because more and more growth angles will overlap.

The trajectory of an interfacial edge during growth (Fig. 1d) can be defined as a function  $r_y = f(r_x)$ , or as its inverse function, relating the variations of the central distances of faces. In the natural co-ordinate system of a crystal section perpendicular to its zone axis it can be measured in two convenient ways. Sequences of well defined straight lines (curve 1, Fig. 1d) can be

expressed by central distances  $r_x$  and the respective angles  $\psi_x$ . In more complicated cases (Vesselinov, Kerestedjian, 1995), measurement of  $r_x$  and the distance  $w_x$  from the face normal to the edge is more practicable. Further on we shall assume that edge paths are measurable with any desired accuracy. Simple geometric relations give  $r_y = \cos\varphi \cdot r_x + \sin\varphi \cdot w_x$  and  $dr_y/dr_x = \cos\varphi + \sin\varphi \cdot (dw_x/dr_x) = \cos\varphi + \sin\varphi \cdot \cot\psi_x$  at any point along the trajectory. Since it is also valid  $dr_y/dr_x = (dr_y/dt)/(dr_x/dt)$ , Laemmlein's equation can be rewritten as  $V_y/V_x = \sin\psi_y/\sin\psi_x = (dr_y/dt)/(dr_x/dt) = \cos\varphi + \sin\varphi \cdot (dw_x/dr_x) = F_{xy}$  at any moment  $t$ , and the problem can be redefined as an inverse kinematic problem in which the functions  $r_x = f_x(t)$  and  $r_y = f_y(t)$  are to be sought if the growth rate ratio function  $(dr_y/dt)/(dr_x/dt) = F_{xy}$  is known from measurements. Of course, with the exception of zero rates, the edge trajectories  $F_{xy}$  give no information about the absolute growth rates of faces.

It is quite evident that in order to solve the problem one has to know, ideally, at least one  $r$  vs.  $t$  function. Yet, if it is correctly found, even in arbitrary, not absolute time units, the evolution of the entire growth morphology can be traced back from the set of all edge trajectories in a crystal. A search for functions, based on crystal growth theories, laboratory experiments and observations in nature, would necessarily require checking up the results against the recorded patterns. The means for that are provided by the program SHAPE 5.0 (Dowty, 1995; see also Vesselinov, 1994) which can model growth after entering the functions  $(dr_y/dt) = F_{xy}(dr_x/dt)$ , etc., derived from the set of  $F_{xy}$ 's and a model function  $(dr_x/dt)$ , by drawing a succession of section polygons at equal, up to 20, time intervals. Examples of the procedure, based on the very scarce measured patterns available in publications, are given in the following sections. Three simple model functions have been used, as follows:

- decelerating mode (DM):  $r_x = k_{x(DM)} t^{1/2}$ ,  $dr_x/dt = k_{x(DM)} t^{-1/2}/2$ ;
- constant-rate mode (CM):  $r_x = k_{x(CM)} t$ ,  $dr_x/dt = k_{x(CM)}$ ;

– accelerating mode (AM):  $r_x = k_{x(AM)}t^2$ ,  
 $dr_x/dt = 2k_{x(AM)}t$ .

The choice of the types of functions will be explained in part II of this study. For the purposes of this discussion it should be noted that the  $k_x$  constants reflect specific crystal surface and environmental factors governing growth.

## Straight edge trajectories

This is the simplest case of edge path patterns and it is also a common phenomenon, characterizing for instance many hourglass structures. Laemmlein's equation becomes  $F_{xy} = \cos\phi + \sin\phi(dw_x/dr_x) = \cos\phi + \sin\phi \cdot \cot\psi_x = K_{xy}$ , where the constant  $K_{xy}$  is defined by the known interfacial angle  $\phi$  and the measured constant angle  $\psi_x$ . The middle column of Fig. 2 shows three patterns obtained by multiplying the DM, CM and AM model functions by one and the same  $K_{xy}$  to derive the other function ( $dr_x/dt$ ). They illustrate the following features.

Straight trajectories represent the important case of processes producing stationary growth forms during which a crystal shape does not change but remains similar to itself (Chernov, 1980). A sequence of straight paths (Fig. 1d,e) marks series of stationary growth forms defined by different rate ratio constants.

Stationary forms indicate that the absolute growth rate functions of faces are of identical type and differ only by some constant measurable factor. In the absence of data on absolute rates, the type of function can be roughly inferred from the variations of the widths of concentric zones (if present) and/or from the size of the crystal, but the results should be regarded as inconclusive and must be verified by further analysis as described in Part II. The three drawings in Fig. 2 illustrate how zone widths vary with time: they decrease from core to rim in DM, increase in AM, and remain constant in CM.

Crystal size is a very important characteristics because it marks the end of growth  $t_e$  at which a central distance has reached a value of  $r_e$ . The effect of the three modes

DM, CM and AM, which would result in a given measured distance  $r_e$ , may be evaluated in two ways: at equal total growth times  $t_e$  compensated by different rate factors  $k_x$ , i.e.  $r_e = k_{x(DM)}t_e^{1/2} = k_{x(CM)}t_e = k_{x(AM)}t_e^2$ , and at different total times with equal growth rate factors, i.e.  $r_e = k_x t_{e(DM)}^{1/2} = k_x t_{e(CM)} = k_x t_{e(AM)}^2$ . The first comparison, aided by further analysis as proposed in Part II, would outline potential differences in the growth controlling factors, and the second one would indicate the relative time limits imposed on the overall process by the three model rates. Both may provide valuable clues as to the probabilities of a process to occur in the particular crystallization environment. For instance, at a rate constant of unity (the second proposition) an  $r_e$  of 4 will need 16 time units in DM, 4 in CM, and 2 in AM, and these large differences may help to choose the most probable mode under the specific natural conditions.

A great number of complex growth patterns in accessory zircon from granitoids has been measured by Vavra (1993) who also used SHAPE for modelling some of them. A particularly impressive illustration of sequences of straight edge paths (reflecting a series of growth events) is his Fig. 8 (Vavra, 1993) which, in terms of this study, uses the growth rate of (101) as a CM model function to represent the growth rates of six other faces by the respective measured constants. The works of that author on zircon morphology, summarized in the quoted paper, treat also the need of statistics and other important problems in the study of internal patterns, and demonstrate the non-trivial implications of their analysis.

## A case of hyperbolic trajectories

In 1968, Kastner, Waldbaum described hourglass patterns in authigenic albite formed in micritic limestone during early diagenesis. They consist of numerous calcite, quartz and calcareous inclusions in the interior which, close to the cores of the euhedral crystals, disappear from the {010} growth pyramids (thus marking a growth event shortly after the start of crystalliza-

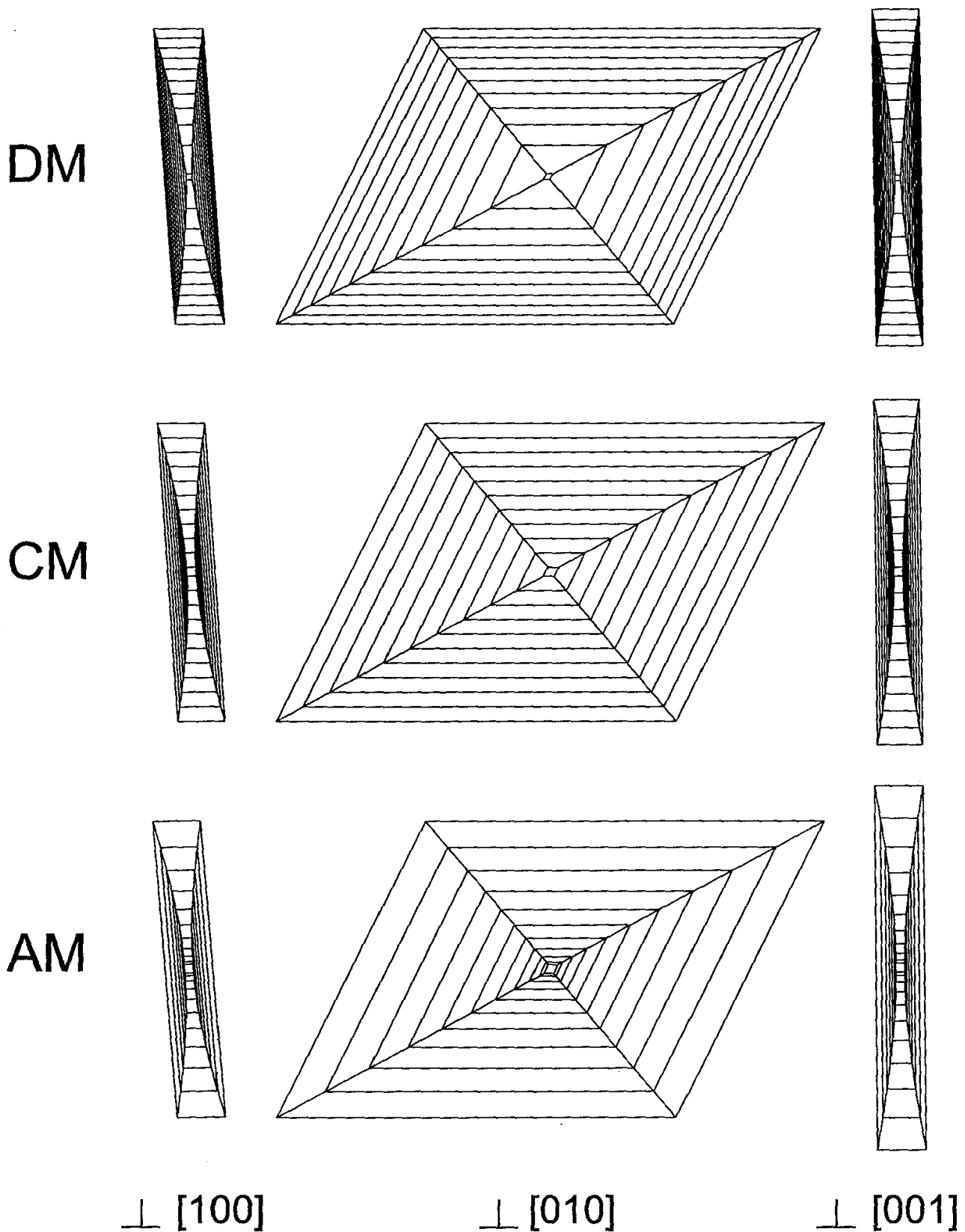


Fig. 2. SHAPE models of a hyperbolic pattern in authigenic albite for the decelerating (DM), constant-rate (CM) and accelerating (AM) growth modes  
 Фиг.2. Модели с SHAPE на хиперболична структура в аутигенен албит в режими на растеж с намаляваща (DM), постоянна (CM) и нарастваща (AM) скорост

tion). The authors describe the surface dividing the inclusion-rich from the inclusion-poor volumes and sketched in their Fig. 5 as a very flat hyperboloid of two-sheets  $r_y^2/f^2 - r_z^2/g^2 - r_x^2/e^2 = 1$ , where  $r_x, r_y, r_z$  run along the normals of (100), (010) and (001) resp., and the constants are  $f \ll g \ll e$ . Along the same directions, the crystals reach up to 1.8, 0.3 and 1.5 mm, resp. Thus, the initial short period, during which all growth pyramids entrapped inclusions at unknown rate ratios, was followed by an abrupt increase of the relative {010} rates under inclusion-free conditions asymptotically approaching constant rate ratios with time. The well defined internal geometry permits the following analysis of growth kinematics with some results shown in Fig. 2.

For the section  $r_z = 0$  we obtain the hyperbola  $r_y^2/f^2 - r_x^2/e^2 = 1$  (asymptote  $r_y = [f/e]r_x$ ) from which we derive  $(dr_y/dt)/(dr_x/dt) = (f^2/e^2)(r_x/r_y)$ , and  $(dr_y/dt) = (f/e)(dr_x/dt)(1 + e^2/r_x^2)^{-1/2}$ . For the section  $r_x = 0$  we have  $r_y^2/f^2 - r_z^2/g^2 = 1$  (asymptote  $r_y = [f/g]r_z$ ), obtaining  $(dr_z/dt)/(dr_y/dt) = (g^2/f^2)(r_y/r_z)$ , and  $(dr_z/dt) = (g/f)(dr_y/dt)(1 - f^2/r_y^2)^{-1/2}$ . For the section  $r_y = 0$ , which is between the two hyperboloid sheets, the relations are  $r_z =$

$[g/e]r_x$ , and  $(dr_z/dt) = (g/e)(dr_x/dt)$ . The unknown ratios  $e : f : g$  can be derived by assuming that the maximum crystal dimensions have been reached in long enough time so that the difference between the respective hyperbola and its asymptote has become negligibly small. We obtain  $2e : 2f : 2g = 1.8 : 0.3 : 1.5 = 6 : 1 : 5$ . Now the model functions DM, CM and AM can be substituted in the above relations to draw test crystals by the computer, experimenting also with various  $k_x$ 's and  $t_e$ 's in them, as proposed in the previous section, to satisfy the boundary conditions imposed by the observed crystal dimensions. The general features of patterns obtained by the three modes are illustrated in Fig. 2 for total growth times 16 in DM, 4 in CM and 2 in AM (compare with the second proposition in the previous section). The small inclusion-rich core formed before the onset of hyperbolic growth is reproduced by the first zone grown at equal rates of the three forms.

A general feature of hyperbolic patterns is that they record growth processes which, in contrast to those discussed already, never produce stationary morphologies although the crystals asymptotically approach them

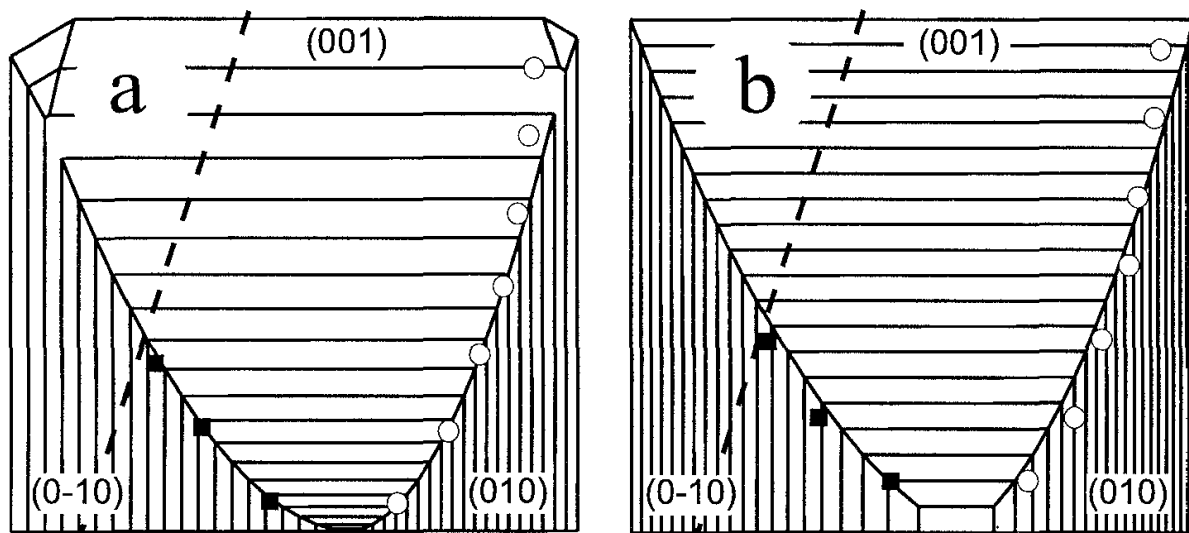


Fig. 3. SHAPE models of a parabolic pattern in titanite: *a* - (010) and (0-10) are in DM resulting in CM of (001); *b* - (010) and (0-10) are in CM resulting in AM of (001). The points measured by Gray (1971) are marked. Dashed line marks the end of the original section

Фиг. 3. Модели с SHAPE на параболична структура в титанавгит: *a* - (010) и (0-10) са в режим DM, който води до режим CM на (001); *b* - (010) и (0-10) са в режим CM, водещ до AM на (001). Маркирани са точките на измерванията на Gray (1971), щриховата линия показва края на пререза в оригиналната фигура

with the increasing size. In this example stationary and non-stationary sections can be directly compared (Fig. 2). The hyperbolas produced by the DM model have sharper noses and flatter, almost linear branches than in the other models. Comparisons with photographs in Fig. 3 of Kastner, Waldbaum (1968) show that most probably it was this mode that controlled the growth of all figured crystals including those of apparently linear sector boundaries. This hypothesis is strengthened by the longer growth times needed by the DM model which agrees with the growth conditions to be expected in such an environment of crystallization as discussed in Part II. Generally, patterns of such well defined and more complex geometries provide much more conclusive evidence than simpler ones and permit to model a growth process in arbitrary time units.

## A parabolic trajectory

In what may be called a pioneer study, Gray (1971) tried to deduce the kinetics of crystal growth of titanite phenocrysts from the (unusual) parabolic shape of their hour-glass structures. The kinematics underlying the pattern was not examined in detail, and presents an interesting problem for the present-day computer-based techniques.

The pattern, shown graphically in Fig. 2 of Gray (1971), is a perfect second-order parabola in the (100) section produced by the growth of (001), (010) and (0-10). As noted by Gray, its symmetry axes are slightly (about 6°) skewed with respect to the orthogonal system of the normals to (010) and (001). Since it was measured in the plane (100), it is also tilted with respect to the zone axis [100] of the three faces by the angle ( $\beta-90^\circ$ ), i.e. about 15° for titanite. Thus, before modelling the pattern by the computer it has to be recalculated in the correct co-ordinate system required by Laemmlein's relation. Gray did not express the curve analytically but careful measurement of the diagram has given  $y = 0.070x^2$  in the original co-ordinates, transformed to  $r_y = 0.091r_x^2 = 0.042r_{-x}^2$  where  $r_y$ ,  $r_x$  and  $r_{-x}$  are the central distances of (001), (010) and

(0-10), resp. The transformation has broken up the original parabola into two parabolic branches reflecting the simple fact that the two symmetry related faces of {010} underwent unequal development and produced a distorted crystal shape, as can be seen in Fig. 2 of Gray (1971). Substitution of the DM model for  $r_x$ , ( $dr_x/dt$ ) in these expressions results in CM along  $r_y$ , and substitution of CM along  $r_x$  produces AM along  $r_y$ . The two models are shown in Fig. 3 to illustrate the unambiguous way in which the correct functions can be found in this case. There are three other important aspects of this example which need some comment.

Kouchi et al. (1983) have reproduced sector zoning and measured the growth rate of clinopyroxenes in laboratory experiments, thus providing data for evaluation of their absolute rates of crystallization in natural environments.

Growth rates of clinopyroxene phenocrysts supply important information about other related contemporaneous processes and the results of Kouchi et al. (1983) have been used for assessing the time period of extrusion of a basalt body (Shimizu, 1990). They become even more important, however, if compared with the rates of the reverse process of dissolution of xenocrysts entrapped by the magma along its way upwards. That follows from the fact that the two processes, growth and dissolution, occur side by side but there are time differences depending on the level in the crust from which the xenocrysts have been extracted. Reaction rims of xenocrysts have been used for assessing the velocity of upward flow (e.g. Zhang et al., 1989), but if the times derived in such studies are compared with those of phenocryst growth they will provide clues as to the source of xenocrysts and will strengthen or weaken hypotheses about the overall process of emplacement and solidification.

The pattern of Gray (1971) demonstrates that the growth process has been continuous, undisturbed during the parabolic growth, the unequal rates of the two {010} faces included. The slower (010) growth has been evidently caused by a weaker supply of nutrient (probably due to



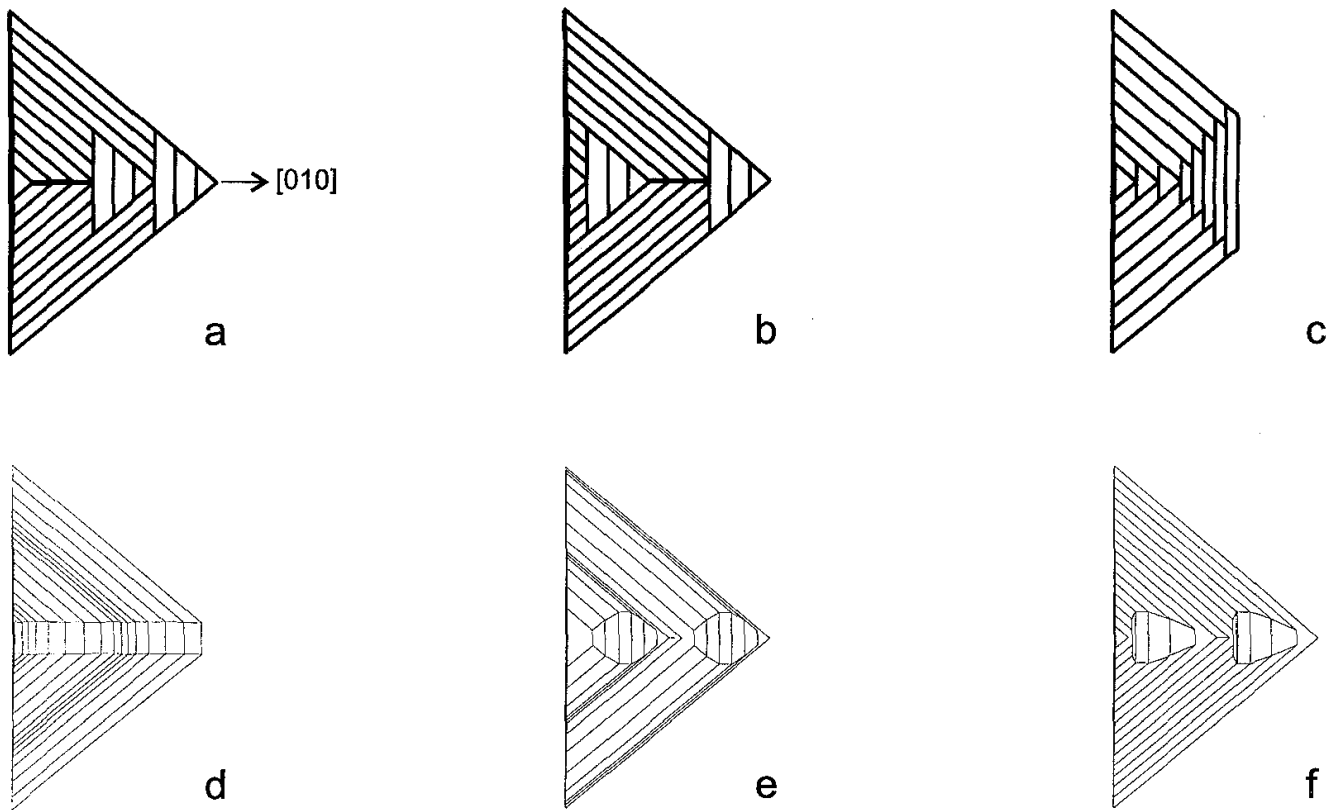


Fig. 4. SHAPE models of periodic patterns: *a, b, c* - „fir-tree“ zonings, where *c* shows the effect of different rate ratios and absolute rates; *d, e, f* - trajectories produced by sine oscillations of growth rates  
 Фиг. 4. Периодични структури, моделирани с SHAPE: *a, b, c* - зоналности тип „елхичка“ като в *c* е показан ефектът от разликите в отношенията и в абсолютните стойности на скоростите; *d, e, f* - траектории, получени със синусоидални колебания на скоростите

another crystal growing closely by), and the cause remained active during the entire period of parabolic growth. If the crystal was not part of a glomerocryst (Gray, 1971, did not comment on that) but an individual crystal, its distorted shape would mean that there was either no flow in the magma body, or the flow was laminar and did not disturb significantly the distances between crystals. Studies based solely on compositional variations (see Paterson, Stephens, 1992, for a relevant discussion) frequently infer events such as sudden forced magma movements from sharp compositional changes. The present example demonstrates that conclusive evidence about flow processes in a magma body can be derived from a careful examination of hourglass

patterns and distorted shapes in phenocrysts during any routine study of thin sections.

## Periodic patterns

Oscillatory zoning is one of the important phenomena under study and debate at present (see Holten et al., 1997, for a view on the current state of the problem). The geometry of patterns seems to be totally ignored though, and this author is unaware of any other measured trajectories in publications besides that in a crystal of hydrothermal arsenopyrite in Vesselinov, Kerestedjian (1995). That pattern is a complex one and requires a separate analysis,

but the simple (001) section of arsenopyrite with (010) growing between (210) and (-210) along [010] has been used again here to illustrate some general features of periodic trajectories in crystals. Since we do not have any  $F_{xy}$  functions now, the alternative procedure of selecting  $(dr_x/dt)$  and  $(dr_y/dt)$  and letting SHAPE create the trajectories has been employed. The program has no special option for periodic functions because of which its „discontinuous growth mode“ has been used entering rates calculated beforehand at intervals of  $\pi/4$  to take the best advantage of the 16 zones available in that option.

In order to express the rates in an oscillating mode (OM), we have superimposed sinusoidal longitudinal variations on another growth rate mode to obtain  $(dr_x/dt) = V_x + A_x \cos \omega t = V_x [1 + (A_x/V_x) \cos \omega t]$ , where  $V_x$  is some growth rate function,  $\omega = 2\pi/T$  is a constant angular velocity, and  $A_x = a_x(\lambda_x/T) = a_x(2\pi\rho_x/T) = a_x(\rho_x\omega)$ , in which  $\lambda_x$  is the wavelength of variations along  $r_x$ ,  $\rho_x$  is the amplitude of sine oscillations, and  $a_x$  is a constant. The magnitude of  $a_x$  is limited by the condition that the growth rate cannot be negative from which it follows  $[1 + (A_x/V_x) \cos \omega t] \geq 0$ , and  $A_x = a_x(\lambda_x/T) \leq V_x$ . At  $a_x = 0$  the oscillations become inactivated.

A convenient procedure in experimenting with OM is first to choose a trajectory  $dw_x/dr_x$  in Laemmlein's relation, then to select functions  $(dr_x/dt)$ ,  $(dr_y/dt)$  producing that trajectory, and finally to superimpose oscillations of chosen wavelengths, amplitudes and phases. In the following examples,  $r_x$  and  $r_y$  run along the normals to (010) and (210), (-210) of arsenopyrite,  $dw_x/dr_x$  are constants, i.e. the edge trajectories are straight lines, and the rate functions  $V_x, V_y$  are also constants (CM). The wavelength of oscillations along  $r_y$  is a projection of that along  $r_x$  ( $\lambda_y = \cos\phi\lambda_x$ ) and the variations are always in phase to simulate the effect of a cause acting simultaneously on all faces.

In the first three very simple examples (Fig. 4a,b,c),  $A_x = A_y = 0$ , and in the half period  $0 \leq \omega t, V_x = 0$  at some constant value of  $V_y$ , whereas in  $\pi \leq \omega t < 2\pi, V_y = 0$  at a con-

stant  $V_x$ . Fig. 4a show oscillations about an edge trajectory of  $dw_x/dr_x = 0$ , and the symmetry of the (001) section turns them into a pattern commonly used to illustrate sector zoning (e.g. Laemmlein, 1948; Sunagawa, 1987) and called „fir-tree zoning“ (e.g. Paterson, Stephens, 1992). The zero absolute rates of faces are readily recognized in such patterns because their outlines are parallel to the faces involved. Inversely, non-parallelism means non-zero rates. In Fig. 4b, (010) is allowed to grow for another three time units before being blocked again, which introduces blank portions in the pattern, i.e. (010) disappear, illustrating the effect of overlapping growth angles, in this case those between (010),(210) and (010), (-210), mentioned in a previous section. Fig. 4c shows the effect of diminishing growth rates and of changes in edge trajectory. In the first six intervals the edge trajectory carrying the oscillations runs parallel to  $r_x$  at  $V_y = \cos\phi V_x$  and  $V_x$  is double that in the remaining intervals, during which the edge trajectory is parallel to  $r_y$  at  $V_y = V_x/\cos\phi$ . It is seen that the diminishing absolute rates produce oscillations of shorter wavelengths and smaller amplitudes which both are measurable quantities and can be analyzed to derive trends in the variation not only of rate ratios, but of absolute rates as well. This property of periodic patterns, lacking in non-periodic ones, makes their study even more important and adds to their significance as natural time-recording devices.

Figs 4d,e,f illustrate sine oscillations superimposed on a trajectory of  $dw_x/dr_x = 0$ . In Fig. 4d,  $A_x/V_x = A_y/V_y = 0.5$  to show that at equal amplitudes the resulting trajectory will be a straight line, adding an OM model of stationary shapes to the already discussed DM, CM and AM models (Fig. 2). In Fig. 4e,  $A_x/V_x = 0, A_y/V_y = 1$ , and in Fig. 4f,  $A_x/V_x = 1, A_y/V_y = 0$ . Note the great difference between the two patterns. It is defined by the geometry of the section (the angle) because both patterns are produced by smooth oscillations of one of the rates at a constant value of the other rate. This difference has two very important implications. First, it shows that the shape

of a given pattern may provide conclusive evidence as to which rate has varied in a specific case (the greater amplitude of (010) rate variations than that of (210),(-210) has already been inferred by an independent but less conclusive analysis in Vesselinov, Kerestedjian,1995). And secondly, nothing in the shape of the (010) „bullets“ in Fig. 4f is suggestive of the smooth oscillations of the (010) growth rate. On the contrary, they are seemingly indicative of saw-toothed changes with abrupt rise and slow fall. Such changes have been envisaged in theories in order to explain compositional patterns in solid solutions (e.g. Ortoleva, 1990). Yet, the example here combined with the compositional pattern in Vesselinov, Kerestedjian (1995) shows that smooth rate oscillations may produce abrupt compositional changes. This non-trivial result may greatly facilitate theoretical treatments of oscillatory zoning.

## Conclusion

Edge paths in crystal sections are direct records of crystal growth kinematics that can be measured and analyzed by Laemmlein's relation to derive a limited number of possible growth histories and to model and assess the probabilities of one or another process to occur under specific natural conditions, as illustrated by the examples covering a wide range of environments: sedimentary, magmatic, and hydrothermal. This source of information becomes even more important when analyzed in terms of crystal growth kinetics as proposed in Part II of this study.

*Acknowledgements* The program SHAPE 5.0 for Windows was generously made available to me by its author Dr. E. Dowty. The study was financially supported by the National Science Fund, Grant H3-434.

## References

Cashman, K. V. 1990. Textural constraints on the kinetics of crystallization of igneous rocks. - In: Nicholls, J., J. K. Russel (Eds) *Modern Methods of Igneous Petrology: Understanding Magmatic Processes*. Reviews

in Mineralogy, **24**, Miner. Soc. Amer. Series, 259-314.

Chernov, A. A. 1980. Processes of crystallization. - In: Chernov, A. A. (Ed.) *Modern Crystallography. III. Crystal Growth*. (Russian Edition) M., Nauka, 7-232. English translation: 1984. Springer Series of Solid-State Sciences, **36**. Berlin-Heidelberg-New York, Springer.

Dowty, E. 1995. SHAPE 5.0 for Windows (personal communication).

Gray, N. H. 1971. A parabolic hourglass structure in titanite. - *Amer. Mineral.*, **56**, 952-958.

Holten, T., B. Jamtveit, P. Meakin, M. Cortini, J. Blundy, H. Austrheim. 1997. Statistical characteristics and origin of oscillatory zoning in crystals. - *Amer. Mineral.*, **82**, 596-606.

Kastner, M., D. R. Waldbaum. 1968. Authigenic albite from Rhodes. - *Amer. Mineral.*, **53**, 1579-1602.

Kouchi, A., Y. Sugawara, K. Kashima, I. Sunagawa. 1983. Laboratory growth of sector zoned clinopyroxenes in the system  $\text{CaMgSi}_2\text{O}_6\text{-CaTiAl}_2\text{O}_6$ . - *Contrib. Mineral. Petrol.*, **83**, 177-184.

Laemmlein, G. G. 1948. Sector structure of crystals. - In: Laemmlein, G. G. 1973. *Morphology and Genesis of Crystals*. Moscow, Nauka, 107-132 (in Russian).

Ortoleva, P. J. 1990. Role of attachment kinetic feedback in the oscillatory zoning of crystals grown from melts. - *Earth-Sci. Rev.*, **29**, 3-8.

Paterson, B. A., W. E. Stephens. 1992. Kinetically induced compositional zoning in titanite: implications for accessory-phase/melt partitioning of trace elements. - *Contrib. Mineral. Petrol.*, **109**, 373-385.

Shimizu, N. 1990. The oscillatory trace element zoning of augite phenocrysts. - *Earth-Sci. Rev.*, **29**, 27-37.

Sunagawa, I. 1987. Morphology of minerals. - In: Sunagawa, I. (Ed.) *Morphology of Crystals, Part B*. Tokyo, Terrapub, 509-587.

Vavra, G. 1993. A guide to quantitative morphology of accessory zircon. - *Chem. Geol.*, **110**, 15-28.

Vesselinov, I. 1994. The SHAPE crystal-drawing computer program as an instrument in research. - *Geochem., Mineral. and Petrol.* (Sofia), **29**, 97-105.

Vesselinov, I. 1997. Preparing oriented single-crystal sections for measurements of internal morphology. - *Geochem., Mineral. and Petrol.* (Sofia), **32**, 117-123.

Vesselinov, I., T. Kerestedjian. 1995. Kinetic aspects of sector zoning in arsenopyrite: a case study. - *Mineral. Petrol.*, **52**, 85-106.

Zhang, Y., D. Walker, C. E. Lesher. 1989. Diffusive crystal dissolution. - *Contrib. Mineral. Petrol.*, **102**, 492-513.

*Accepted April 11, 1998*  
*Приета на 11.04. 1998 г.*